-Technical Paper-

RESISTANCE AGAINST MICROCRACKING OF SLAG CONCRETE WITH HIGH ALITE CEMENT ANALYZED BY AE WITH NEW WAVE-GUIDE

Huynh Phuong NAM[*1], Akira HOSODA[*2]

ABSTRACT

Acoustic emission (AE) technique with a newly developed wave-guide and mechanical tests were applied to investigate microcracking in slag concrete in various periods during high temperature history simulating steam curing. The effectiveness of the new wave-guide which could reduce the effects of attenuation was confirmed in collecting AE signals in concrete in very young ages, especially for concrete with high w/b. This study also revealed the effect of high alite cement on improving the resistance against microcracking of slag concrete.

Keywords: microcracking, AE, slag concrete, new wave-guide, early age, high alite cement

1. INTRODUCTION

Thermal cracking in concrete in early ages is the concern of many studies. Microscopic thermal stress appears significantly in concrete in case of massive concrete and heat curing, due to the incompatibility in deformation between aggregate and matrix. Microscopic thermal stress leads to microcracking inside concrete even without the application of external load. In expansion period during temperature changing, once stress exceeds the bonding capacity between aggregate and cement paste, separation cracks occur around aggregates at interface transition zone (ITZ). In shrinkage stage, when stress becomes larger than tensile strength of mortar, cracks are expected to generate in matrix.

Nowadays, concrete made with ground granulated blast furnace slag (GGBFS) has been prevailingly used all over the world, especially in Japan. Despite many advantages such as high compressive strength, better workability, environmental conservation and high durability, it is also subjected to severer microcracking than normal concrete.

Due to its sensitivity, acoustic emission (AE) technique has been widely used to detect deterioration of hardened concrete. Analyzing various AE parameters can reveal the characteristics of microcracks. By using a wave-guide embedded inside concrete, microcracking in slag concrete in early ages was analyzed [1]. However, attenuation of acoustic wave in high moist medium was a problem. In this study, a combination of AE technique using a new-shaped wave-guide with mechanical tests was employed to understand the characteristics of microcracks in slag concrete subjected to temperature variation in early ages. The crack resistance of slag concrete with newly developed high alite cement (alite-rich) was also investigated.

2. EXPERIMENTAL PROGRAM

2.1 Acoustic emission system

Two-channel AE system and R15-Alpha sensors, which are for general purpose in temperature interval ranging from -65°C to 177°C, were used. The experimental system of AE tests is shown in Fig. 1. In each test, two sensors were coupled with a sensor seat located at the top of a stainless steel wave-guide, which was embedded in the specimen. The details of our newly developed wave-guide are explained in section 2.2. The specimen with the wave-guide and the sensors were put into a temperature controlling chamber.

Many efforts were carried out to dispose external noises occurring during the tests. Son and Hosoda were successful in using damping buffer to isolate the vibration deriving from the dynamic parts of the temperature controlling chamber and the operation of other surrounding machines [2]. With a threshold value of 40 dB, sound from the outside ambient transmitting through air was rejected. All sensors, pre-amplifiers, and connectors were covered by alumina sheets to discard the effect of electric pulses coming from electrical facilities.

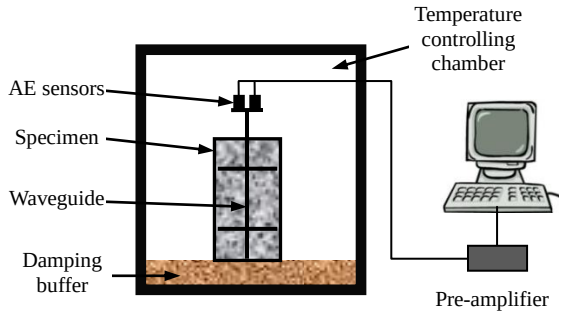

Fig. 1 AE testing system

*1 PhD student, Institute of Urban Innovation, Yokohama National University, JCI member
*2 Associate Professor, Dr.Eng., Institute of Urban Innovation, Yokohama National University, JCI member

Cylindrical tin moulds with 100mm in diameter and 200mm in height were used for all the tests. To eliminate noises induced from the friction between concrete and the mould under temperature variation, the inside face of the mould was covered with 0.5mm thick teflon sheet (Fig. 2a).

Time for preparing the specimen including installation of wave-guide and sensors was around 30 minutes. Right after finishing preparation, concrete was sealed by polyethylene film inside the mould and placed in the temperature controlling chamber, which had been maintained at 20°C. The heating began at 2 hours after adding water into the mix. Temperature regime applied for the specimens is shown in Fig. 3. The record of AE signals started at 1.5 hours after mixing.

2.2 Wave-guide

The acoustic waves were measured after one hour and a half from mixing. Since concrete is in plastic form in early ages, AE sensors cannot be coupled directly on the surface of the specimens. To deal with this problem, AE wave-guide (Fig. 4a) was applied by Son and Hosoda. Through this wave-guide, acoustic waves from cracks inside specimens were collected to AE sensors. This wave-guide was a stainless steel rod with 250mm length and 4mm diameter, with a sensor seat on the top [1]. In case of concrete with water to binder ratio of 0.5; however, this wave-guide did not work properly due to the attenuation of acoustic wave in a high moisture content ambient [3].

In order to solve the matter of attenuation, a new-shaped wave-guide was employed in this research (Fig. 4b). It was made from a stainless steel plate with 4mm thickness. The section of the wave-guide is square with dimension of 4x4mm. The rod is 250mm in length with two horizontal bars located at 50mm and 150mm from the bottom. On the top, 25x50mm plate is perpendicularly bent to the vertical rod making a sensor seat. Since two sensors can be coupled on the seat at a time, only one specimen was used in each experiment. The method for coupling sensors to the sensor seat is found in elsewhere [1]. The effectiveness of the new wave-guide will be discussed in detail in section 3.1.

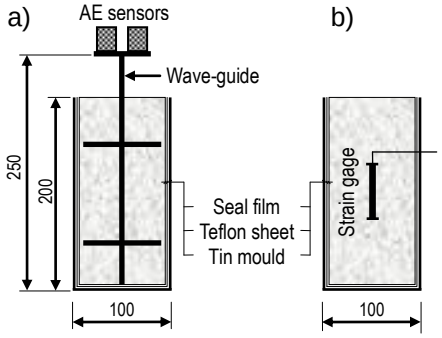

Fig. 2 Specimen preparation for (a) AE test, and (b) CTE test

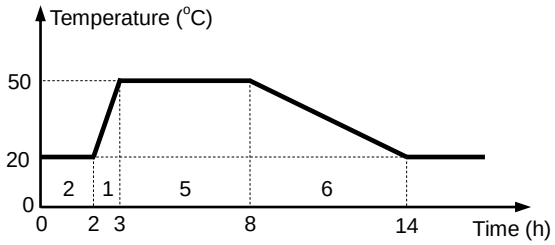

Fig. 3 Temperature regime simulating heat curing

2.3. CTE measurement

Coefficient of thermal expansion (CTE) of mortar was measured by using an embedded I-shaped strain gage. The strain gage was PMFL-60-2LT type with diameter of 4mm and with length of 60mm. Fig. 2b describes the method of measuring the CTE of mortar. Two specimens of one mix were tested at the same time and the mean value was taken. Tests of CTE were conducted at the age of 24 hours after heat curing. Specimens were heated from 20°C to 50°C in two hours, and maintained at 50°C for two hours, and then cooled down to 20°C in two hours. CTE of mortar was calculated separately for heating and cooling stages and the average was taken.

In case of coarse aggregates, CTEs were directly measured on the particles. The surfaces in three orthogonal directions of one particle were ground to have smooth surface and flat-type strain gauges FLG-1-11 with 1mm length were attached (Fig. 5). The temperature regime was the same as that used for mortar. The particles were sealed to prevent evaporation. Three large-size particles of each type of coarse aggregate were used in a test and then the average value was calculated.

2.4. Direct tensile strength test

Direct tensile strength of concretes and mortars were investigated at the age of one day following heat curing. Specimens were cylinders with 100mm diameter and 100mm height. The method for the test was proposed by Son and Hosoda [1].

2.5. Materials and mix proportions

In this study, three types of binder were used. They are Ordinary Portland Cement (OPC), High Alite Cement (HAC), and GGBFS. HAC is a newly developed special cement with higher content of alite ($3CaO.SiO_2$) and lower content of belite ($2CaO.SiO_2$) than in OPC [4]. However, total calcium silica portions of the two

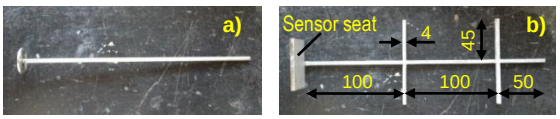

Fig. 4 AE waveguide: (a) previous, and (b) current

Fig. 5 Measurement of CTE of coarse aggregate

cements are equivalent. Main compounds of cements and chemical composition of binders are presented in Table 1 and Table 2, respectively.

In the research, two types of aggregate were used: crushed limestone and crushed andesite with the same maximum particle size of 19mm. Fine aggregate was pit-sand. Two water-to-binder ratios (w/b) 0.3 and 0.5 were used, and super plasticizer (SP) was used for low w/b mix (0.3). Mix proportions of mortar and concrete are presented in Table 3. In all the proportions, 50% of the cement was replaced by GGBFS. Proportions of mortar were calculated from respective concretes by removing coarse aggregates while keeping the proportion of other components. Before mixing, all the materials were stored in a curing room with temperature of around 20°C.

3. RESULTS AND DISCUSSION

After mixing, under temperature variations due to the hydration of binders and heat curing, the volume of aggregate or mortar will be changed. Due to the difference in CTE, as shown in Fig. 6, and due to autogenous shrinkage of mortar, the incompatibility in deformation between mortar and aggregate is induced resulting in microcracking in concrete. In the temperature increasing period (up to 7 hours from mixing), expansion of mortar is larger than that of coarse aggregates, leading to separation at ITZ around aggregate particles. This type of deterioration is defined as separation crack.

In the temperature decreasing period, the contraction of coarse aggregates is smaller than that of mortar and tensile stress is generated in mortar. The level of this tensile stress depends on the size of coarse aggregate and the distance from the center of aggregate. The larger the size of aggregate is and the smaller distance from the center of the aggregate is concerned, the larger this tensile stress becomes [5] [6]. If the tensile stress exceeds the tensile strength of mortar, cracks will appear in mortar in the perpendicular direction to ITZ that are called mortar cracks.

3.1 Effectiveness of new-shaped wave-guide

Since the sensor seat of the new-shaped wave-guide is large enough to couple two sensors simultaneously, the accuracy of measurement is remarkably improved.

In previous researches, the numbers of AE hits of concrete with w/b of 0.5 were significantly smaller than those of 0.3 [1]. One of the main reasons is the attenuation of acoustic waves in a high moist medium [7]. In this study; however, the result was reverse. Compared with concretes with w/b of 0.3, concretes with w/b of 0.5 presented much larger cumulative AE hits, particularly in the expansion period (Fig. 7).

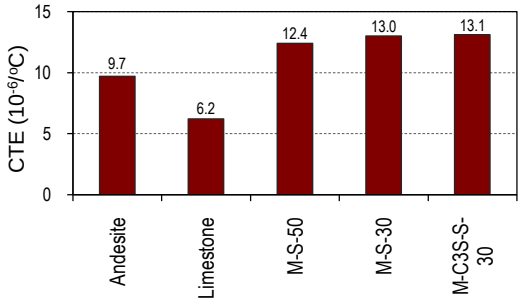

Fig. 6 CTE of mortars and coarse aggregates

Table 1 Main compounds of cements

Cement	Main compounds (%)			
	C_3S	C_2S	C_3A	C_4AF
OPC	59.88	13.52	8.99	9.24
HAC	68.36	2.57	8.91	8.66

Table 2 Chemical composition and physical properties of binders

Binder	Chemical composition (%)								Density (g/cm^3)	Specific area (cm^2/g)
	SiO_2	Al_2O_3	Fe_2O_3	CaO	MgO	SO_3	Na_2O	K_2O		
OPC	20.36	5.33	3.04	64.09	1.50	2.13	0.28	0.36	3.16	3310
HAC	18.76	5.18	2.85	64.16	1.88	3.97	0.42	0.38	3.11	5480
GGBFS	32.3	14.2	0.31	43.4	5.7	1.93	0.26	0.27	2.90	4030

Table 3 Mix proportions

Mixture	Water (kg/m^3)	OPC (kg/m^3)	HAC (kg/m^3)	GGBFS (kg/m^3)	Pit-sand (kg/m^3)	Lime stone (kg/m^3)	Andesite (kg/m^3)	SP (kg/m^3)	w/b ratio
M-S-30	251	418	-	418	1229	-	-	4.2	0.3
M-C_3S-S-30	250	-	417	417	1225	-	-	5.8	0.3
M-S-50	265	265	-	265	1454	-	-	-	0.5
C-S-L20-30	165	275	-	275	810	838	-	2.8	0.3
C-S-A20-30	165	275	-	275	810	-	816	2.8	0.3
C-C_3S-S-L20-30	165	-	275	275	808	836	-	3.9	0.3
C-C_3S-S-A20-30	165	-	275	275	808	-	814	3.9	0.3
C-S-L20-50	165	165	-	165	904	936	-	-	0.5
C-S-A20-50	165	165	-	165	904	-	911	-	0.5

Analysis of amplitude distribution of microcracks (Fig. 8) shows that microcracks in concrete with w/b of 0.5 occurred remarkably at low amplitude. Nearly 50% of them occurred in the range of 40dB to 42dB and 80% in the range of 40dB to 45dB, while in the case of w/b of 0.3, those percentages were just 25% and 50%, respectively. In very early ages, the amount of free water remaining in concrete with w/b of 0.5 is so large. When acoustic waves transmitted through out such a moist medium, attenuation caused drastic decreasing in amplitude. By using two additional horizontal bars, the distances from cracking points to the wave-guide became shorter and hence the effect of attenuation must have been significantly reduced.

The comparison of AE hits between the former wave-guide and the new one in concrete with w/b of 0.5 is presented in Fig. 9. Number of hits detected by the new wave-guide was considerably higher than that recorded by the old one. It can be clearly said that the new one is more effective.

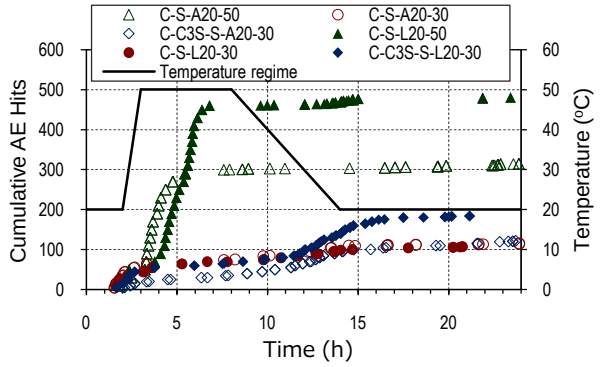

Fig. 7 Development of AE hits during heat curing

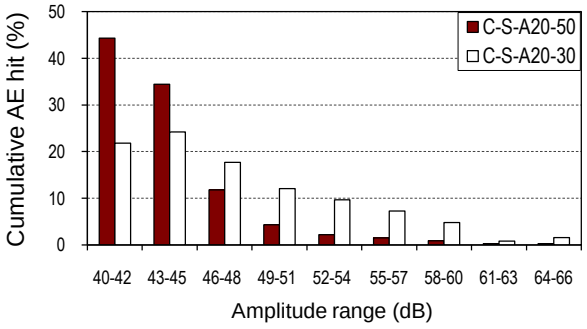

Fig. 8 Amplitude distribution of microcracks

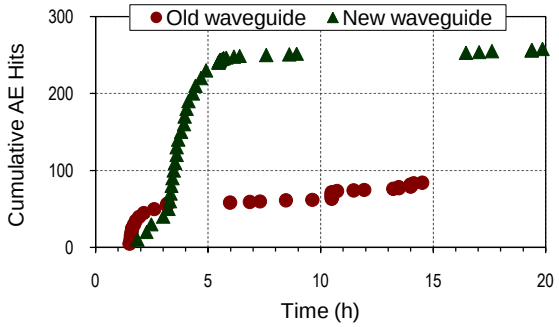

Fig. 9 Comparison of new and old wave-guide in C-S-A20-50

3.2 Characterizing microcracking

Microcracks were generated in concrete during both temperature increasing and decreasing periods of heat curing. Nevertheless, characteristics of them were much different in each stage of curing and in each type of concrete.

(1) Microcracks in expansion period

During the temperature increasing period, separation cracks occurred. In concrete with w/b of 0.5, the number of AE hits was remarkably larger than those of 0.3 (Fig. 7) although the expansion of mortar with w/b of 0.5 in this stage was a bit smaller than the others (Fig. 10). This may indicate that the bonding capacity of mortar with w/b of 0.5 with coarse aggregate was weaker than that of mortar with w/b of 0.3. The reason was that the amount of water, which had not been consumed yet during hydration process of binders, was larger and the remained water made a layer around the surface of coarse aggregate due to bleeding, etc. This water layer decreased the bond strength between matrix and coarse aggregate leading to separation cracks around coarse aggregate particles.

In spite of the fact that number of AE hits in expansion stage of C-S-L20-50 was huge (Fig. 11a), the respective cumulative energy was so small (Fig. 11b). This implies that many microcracks were generated but these cracks appeared at very low stresses.

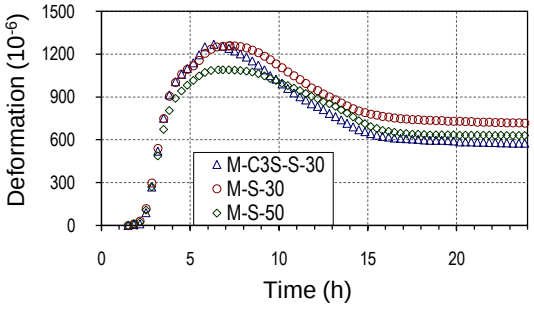

Fig. 10 Total deformation of mortar

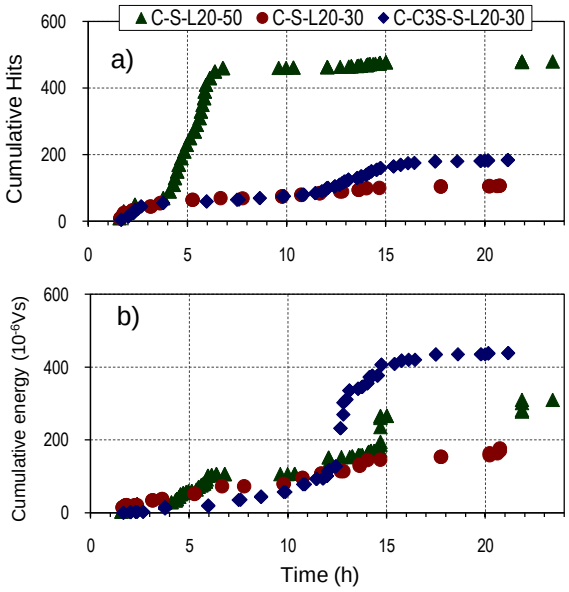

Fig. 11 Development of (a) AE hits and (b) energy of concretes made of limestone

Considering concretes with w/b of 0.3 but different types of cement, the numbers of microcracks in both cases with OPC and HAC were small and the level of deterioration was also small (Fig. 11). The explanation for this is the good bonding capacity between mortar with w/b of 0.3 and aggregates.

(2) Microcracks during shrinkage period

In this stage, mortar was shrinking and mortar cracks were generated due to the incompatibility in deformation between mortar and coarse aggregate. Net shrinkage is defined as the total shrinkage from the peak expansion consisting of both autogenous and thermal shrinkages [8]. Fig. 12 compares net shrinkage of mortars. Mortar with HAC showed the largest net shrinkage and this can be correlated to microcracking magnitude of the respective concrete. In concrete C-C_3S-S-L20-30, the number of microcracks and cumulative energy was higher than in other types of concrete (Fig. 11). However, degree of deterioration in HAC concrete was similar to that in OPC. Fig. 13 below illustrates this idea: the energy rate per hit of two concretes was similar.

Although the cumulative AE hits in temperature decreasing period of C-S-L20-50 was very low, energy rate per hit was high (Fig. 13). It means that in concrete with w/b of 0.5, a few numbers of cracks were generated in the decreasing period, but each crack happened at a high stress. As mentioned above, it can be suggested that these mortar cracks just appeared around large size coarse aggregate.

(3) Classification of crack mode in concrete with w/b of 0.5

Rise time in milliseconds over peak amplitude in volts (RA value) and average frequency have been applied to classify microcracking modes [9]. Cracks in tensile mode tend to have higher average frequency and smaller RA value while longer rise time and often higher peak amplitude were observed in shear mode [10]. The comparison of microcracking mode in two different curing stages of C-S-A20-50 is clarified in Fig. 14. Most of cracks in two stages belonged to tensile mode. In temperature increasing period; however, some microcracks were in shear mode. These cracks were generated between 3.1 hours and 3.6 hours after mixing. It can be explained that in concrete with high w/b in a very early age, cement paste is not sufficiently hardened. In such an unhardened stage, slippages between coarse aggregate and matrix must have led to shear-mode microcracks.

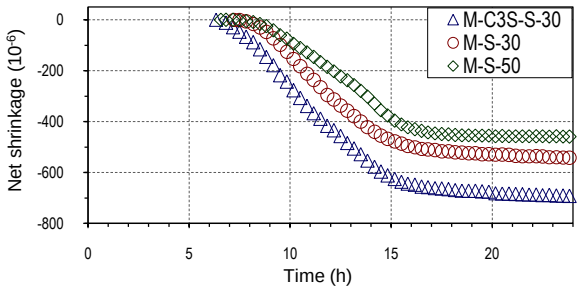

Fig. 12 Net shrinkage of mortar

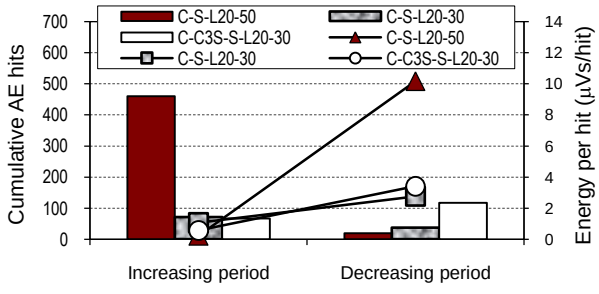

Fig. 13 Cumulative AE hits (columns) and energy rate per hit (dots)

3.3 Resistance against microcracking of slag concrete with high alite cement

Further investigation about tensile strength of concretes and respective mortars revealed some interesting characteristics of HAC. As shown in Fig. 15, although tensile strength of M-S-30 was a bit smaller than that of M-C_3S-S-30, tensile strengths of slag

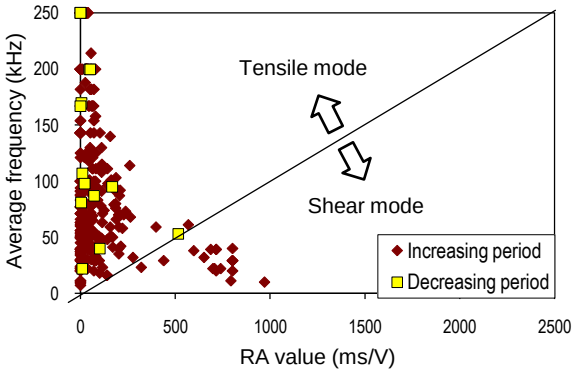

Fig. 14 Classification of crack mode of C-S-A20-50

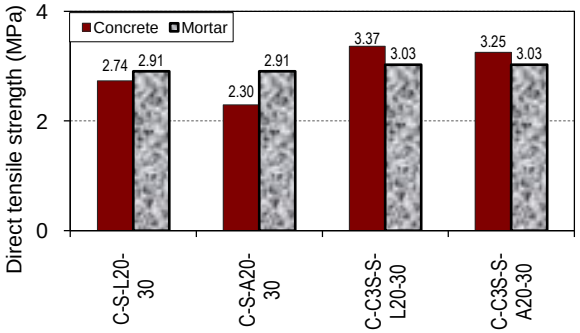

Fig. 15 Direct tensile strength of concrete and respective mortar

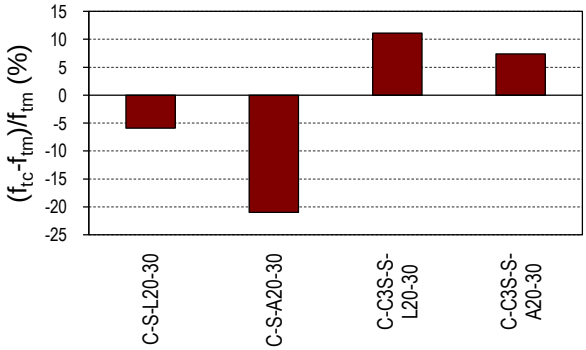

Fig. 16 Tensile strength rate of concrete and respective mortar

concretes with HAC were much higher than those of slag concretes with OPC. Moreover, with HAC, tensile strengths of all concretes were larger than respective mortar. Conversely, in case of OPC, tensile strength of mortar was higher than those of concrete. The degree of difference between tensile strength of concrete and respective mortar made of two types of cement is clearly presented in Fig. 16. It can be said that HAC improved the resistance against microcracking in slag concrete.

The effectiveness of HAC in improving resistance against microcracking may be explained by the role of $Ca(OH)_2$. In hydration of cement, C_3S produces three times as much $Ca(OH)_2$ as is formed by the hydration of C_2S [11]. Therefore, HAC will create more $Ca(OH)_2$ than OPC in hydration. In contrast to C-S-H, $Ca(OH)_2$ is a well-crystallized material with a definite stoichiometry. Distributed $Ca(OH)_2$ crystals might have become a kind of buffers to prevent propagation of microcracking. However, to grasp the role of HAC in improving the resistance against microcracking, more investigations need to be conducted.

Considering the type of aggregate, slag concretes with limestone showed the better direct tensile strength than those with andesite in both case OPC and HAC (Fig. 15) despite of the fact that more microcracks were generated in slag concrete with limestone (Fig. 7) and physical bonding capacity between aggregate and mortar of limestone is smaller than that of andesite due to its polish texture. Furthermore, compared with the previous research [2], although tensile strength of OPC concrete with andesite had a similar value, that with limestone in this study was much higher. This may be partly because the difference of CTEs between limestone and andesite in this research was not so large compared to the previous research. Another reason of higher strength of slag concrete with limestone than that with andesite is chemical reaction between matrix with slag and the surface of limestone aggregate [12].

4. CONCLUSIONS

The main conclusions obtained in this study are the followings:

1. With two additional horizontal bars, a new-shaped wave-guide showed a better performance in detecting AE in concrete in very young ages. It was very effective in concrete with high w/b ratio.
2. For concrete with w/b of 0.5, there were many separation cracks in expansion period but the cracks were small. Conversely, a few severe mortar cracks occurred around large size coarse aggregate during shrinkage stage. These mortar cracks led to low tensile strength of concrete. Most of microcracks in both two periods were in tensile mode.
3. High alite cement can improve resistance against microcracking of slag concrete. Chemical reaction between limestone and slag mortar may have occurred and resulted in the higher resistance of concrete with limestone.

ACKNOWLEDGEMENT

The authors show sincere gratitude to DC CO., LTD for their supplying High Alite Cement for our research.

REFERENCES

[1] Son, H. N. and Hosoda, A., "Detection of Microcracking in Concrete Subjected to Elevated Temperature at Very Early Age by Acoustic Emission," *Journal of Advanced Concrete Technology*, Vol. 8, 2010, pp.201–211

[2] Son, H. N., Hosoda, A., and Watanabe, T., "Characterization of microcracking in very early age concrete subjected to elevated temperature by AE," *Proceeding of JCI Annual Convention*, Vol.32, 2010, pp.323–328

[3] Landis, E. N. and Shah, S. P., "The influence of microcracking on the mechanical behavior of cement based materials," *Advanced Cement Based Materials*, Vol.2, May, 1995, pp.105–118

[4] Hashimoto, A., Asai, S., Koibuchi, K., and Mizobuchi, T.,"Properties of high alite cement", *Annual Meeting of JCA*, Vol.66, 2012 (in Japanese)

[5] Tsiskreli, G. D. and Dzhavakhidze, A. N., "The effect of aggregate size on strength and deformation of concrete," *Power Technology and Engineering*, Vol.4, Jun., 1970, pp.448–453

[6] Elices, M. and Rocco, C. G., "Effect of aggregate size on the fracture and mechanical properties of a simple concrete," *Engineering Fracture Mechanics*, Vol.75, Sep., 2008, pp.3839–3851

[7] Aggelis, D., Polyzos, D. and Philippidis, T., "Wave dispersion and attenuation in fresh mortar: theoretical predictions vs. experimental results," *Journal of the Mechanics and Physics of Solids*, Vol.53, Apr., 2005, pp.857–883

[8] Yang, Y., Sato, R. and Kawai, K., "Autogenous shrinkage of high-strength concrete containing silica fume under drying at early ages," *Cement and Concrete Research*, Vol.35, Mar., 2005, pp.449–456 (in Japanese)

[9] Aggelis, D. G., "Classification of cracking mode in concrete by acoustic emission parameters," *Mechanics Research Communications 38*, 2011, pp.153–157

[10] Ohno, K. and Ohtsu, M., "Crack classification in concrete based on acoustic emission," *Construction and Building Materials*, Vol.24, Dec., 2010, pp.2339–2346

[11] Neville, A. M., "Properties of Concrete," John Wiley & Sons, 1996, pp.867-869

[12] Kodama, A., Hosoda, A., Son, H.N., and Ono, A., "Properties in compression and tension of concrete with GGBFS subjected to high temperature history", *Proceedings of the JCI*, Vol.30, No.1, 2008, pp.363-368 (in Japanese)